HHS Public Access

Author manuscript

Sci Transl Med. Author manuscript; available in PMC 2018 December 31.

Published in final edited form as:

Sci Transl Med. 2017 June 21; 9(395): . doi:10.1126/scitranslmed.aam5434.

VP4- and VP7-specific antibodies mediate heterotypic immunity to rotavirus in humans

Nitya Nair[1,2,*], **Ningguo Feng**[1,3], **Lisa K. Blum**[1,2], **Mrinmoy Sanyal**[1,3], **Siyuan Ding**[1,3], **Baoming Jiang**[4], **Adrish Sen**[1,3], **John M. Morton**[5], **Xiao-Song He**[1,3], **William H. Robinson**[1,2,3], and **Harry B. Greenberg**[1,2,3,†]

[1]Department of Medicine, Stanford University School of Medicine, Stanford, CA 94305, USA.

[2]Department of Microbiology and Immunology, Stanford University School of Medicine, Stanford, CA 94305, USA.

[3]VA Palo Alto Health Care System, Palo Alto, CA 94304, USA.

[4]National Center for Immunization and Respiratory Diseases, Centers for Disease Control and Prevention, Atlanta, GA 30333, USA.

[5]Department of Surgery, Stanford University School of Medicine, Stanford, CA 94305, USA.

Abstract

Human rotaviruses (RVs) are the leading cause of severe diarrhea in young children worldwide. The molecular mechanisms underlying the rapid induction of heterotypic protective immunity to RV, which provides the basis for the efficacy of licensed monovalent RV vaccines, have remained unknown for more than 30 years. We used RV-specific single cell–sorted intestinal B cells from human adults, barcode-based deep sequencing of antibody repertoires, monoclonal antibody expression, and serologic and functional characterization to demonstrate that infection-induced heterotypic immunoglobulins (Igs) primarily directed to VP5*, the stalk region of the RV attachment protein, VP4, are able to mediate heterotypic protective immunity. Heterotypic protective Igs against VP7, the capsid glycoprotein, and VP8*, the cell-binding region of VP4, are also generated after infection; however, our data suggest that homotypic anti-VP7 and non-neutralizing VP8* responses occur more commonly in people. These results indicate that humans can circumvent the extensive serotypic diversity of circulating RV strains by generating frequent heterotypic neutralizing antibody responses to VP7, VP8*, and most often, to VP5* after natural

†Corresponding author. hbgreen@stanford.edu.
*Present address: Aduro Biotech, Berkeley, CA 94710, USA.

Author contributions: N.N. designed and conducted experiments, analyzed data, and wrote the manuscript. N.F., L.K.B., M.S., S.D., and A.S. conducted experiments. B.J. isolated and characterized CDC-9 TLPs. J.M.M. provided tissue. X.-S.H. provided feedback. W.H.R. provided access to Ab repertoire analysis. H.B.G. conceived the study and helped write the manuscript.

Competing interests: W.H.R. owns equity in Atreca. The findings and conclusions in this report are those of the authors and do not represent the official positions of the CDC. N.N., N.F., L.K.B., M.S., W.H.R., and H.B.G. are inventors on a pending patent application (PCT/US2016/041613) held/submitted by Stanford University that covers heterotypic antibodies specific for human rotavirus. The other authors declare that they have no competing interests.

Data and materials availability: Sequence data sets used in this paper are listed in table S6.

SUPPLEMENTARY MATERIALS
www.sciencetranslationalmedicine.org/cgi/content/full/9/395/eaam5434/DC1

infection. These findings further suggest that recombinant VP5* may represent a useful target for the development of an improved, third-generation, broadly effective RV vaccine and warrants more direct examination.

INTRODUCTION

Human rotaviruses (RVs) are the leading global cause of severe diarrhea in infants and young children (1). Two effective RV vaccines, the pentavalent RotaTeq (Merck) and the monovalent Rotarix (GlaxoSmithKline), are recommended by the World Health Organization for worldwide use in young children. Other monovalent RV vaccines are licensed for use in India, Vietnam, and China. The mechanisms by which monovalent vaccines impart heterotypic or serotype cross-reactive immunity against multiple human RV serotypes are unknown. The elucidation of these mechanisms is critical for the development of improved, next-generation RV vaccines needed in developing countries where the efficacy of current licensed, live attenuated vaccines is lower than in developed countries (2).

RVs are nonenveloped, double-stranded, segmented genome RNA viruses with a triple-layered protein (TLP) capsid composed of two surface proteins (VP4 and VP7) and a major inner protein (VP6). RVs infect mature enterocytes of the small intestine. Virus entry and infectivity are increased by proteolytic cleavage of the trimeric attachment protein VP4 to yield its stalk (VP5*) and globular head (VP8*). VP8* mediates cell attachment; VP5* facilitates cell membrane penetration. VP7 is a trimeric calcium-binding surface glycoprotein (3).

Sequence divergence and reassortment of the genes encoding VP4 and VP7 result in great serotypic diversity worldwide among the circulating human RV strains and a binary classification system including G (VP7) and P (VP4) serotypes and/or genotypes. In children, protection against RV infection is mediated primarily by neutralizing antibodies (Abs) that target epitopes on VP4, VP7, or both (4). The near-atomic structure of neutralizing epitopes on VP4 and VP7 from animal and human RVs has been elucidated (5–8). Most isolated murine VP7-specific neutralizing monoclonal antibodies (mAbs) are serotype-specific; however, the antigenic region (1) containing amino acids 94 to 99 is targeted by heterotypic and homotypic neutralizing mAbs (9). VP5* is the target of heterotypic and homotypic murine mAbs; heterotypic epitopes on VP4 have been mapped to antigenic region II at amino acids 392 to 433 (11, 12). In contrast, multiple murine neutralizing mAbs to VP8* appear to be primarily serotype-specific (10, 13).

Epidemiologic and clinical studies demonstrate that heterotypic protective immunity is generated after a single RV infection (14) or immunization (15, 16). The molecular basis for protective immunity after monotypic exposure is unknown. Individual anti-VP4 and anti-VP7 Ab molecules generated after monotypic RV infection or immunization could mediate broad-based protection to new serotypes. This hypothesis is supported by the comparable efficacy of the monovalent Rotarix and the pentavalent RotaTeq vaccines (2). Alternatively, heterotypic immunity could be generated by an array of individual Ab molecules, each with restricted specificity against individual RV G or P type. Only one previous study examined the serotypic specificity of human anti-VP4 and anti-VP7 mAbs. In it, two heterotypic VP4

(VP8*) mAbs and a single homotypic VP7 mAb were identified (17). An additional hypothesis is that Abs to a shared common internal protein epitope on the RV virion (such as VP6) may provide heterotypic protection in vivo, although they lack neutralizing activity in traditional in vitro assays (18, 19).

Here, we demonstrate that individual human mAbs, induced after natural infection and specific for either VP4 (primarily VP5*) or VP7, mediate potent heterotypic neutralizing activity, whereas most of the human VP8*-binding mAbs are inactive in a traditional in vitro neutralization assay. These findings reveal a molecular basis for the broad-based, serotype cross-reactive, heterotypic protection against RV observed in humans.

RESULTS

Isolation of RV TLP-specific intestinal B cells by flow cytometry

Intestinal B cells were isolated from adults undergoing bariatric surgery for obesity. Virtually all adults in the world have been infected with RV at least once and therefore have a notable frequency of RV-specific B cells in the intestine at steady state (20). To identify intestinal B cells that recognize RV by flow cytometry, we used purified TLPs (CDC-9, G1P[8]) labeled with Cy5 as bait. The structural integrity of the labeled TLPs was confirmed by electron microscopy (fig. S1A). The binding specificity of TLP-Cy5 to B cells expressing surface VP4- or VP7-specific immunoglobulin (Ig) was assessed using mouse hybridomas specific for VP6 and for serotypically distinct VP4s (P[8] or P[3]) and VP7s (G1 or G3) (18, 21). CDC-9 TLP-Cy5 stained G1- and P[8]-specific hybridomas with mean fluorescence intensity (MFI) of 9800 + 71 and 12801 ± 282 (MFI ± SD), respectively, but not G3- or P[3]-specific hybridomas (fig. S1, B and C). Preincubation of G1- or P[8]-specific hybridomas with unlabeled TLPs reduced TLP-Cy5 binding to both hybridomas (fivefold for G1 and sevenfold for P[8]). The binding of CDC-9 TLP-Cy5 to VP6-specific hybridomas (737 ± 89, MFI ± SD) was lower than to G1-specific hybridomas (13-fold) or P[8]-specific hybridomas (17-fold). Treatment of the TLP-Cy5 with EDTA, which dissociates the outer capsid proteins, resulted in a 24-fold increase in VP6-specific hybridoma binding (fig. S1C). Preincubation of VP6-specific hybridomas with unlabeled TLPs reduced TLP-Cy5 staining by twofold. Blocking with unlabeled TLPs reduced TLP-Cy5 staining of total intestinal IgA$^+$ Ab-secreting cells (ASCs) (10-fold) and IgA$^-$ ASCs (4-fold) (fig. S1, D and E).

TLP-Cy5 was next used to isolate RV-reactive B cells from proximal jejunum resections from five adults (Fig. 1 and table S1). ASCs were identified by CD20$^{lo/-}$CD27^{hi}CD38^{hi} surface expression (Fig. 2A) as described (20, 22). Most intestinal ASCs were IgA$^+$ (median frequency, 59.4%); IgA$^-$ ASCs were detected at a frequency of 40.6%. Within the ASCs, most TLP binding was detected among IgA$^+$ ASCs at a frequency of 0.13% (0.09 to 1.30%). Some TLP-binding cells were observed among IgA$^-$ ASCs (0.01%; 0.00 to 0.04%) (Fig. 2B). An enzyme-linked immunospot (ELISPOT) assay using RV double-layered particles (DLPs) as capture antigen, which detects Abs directed at VP6, confirmed that all donors had detectable Ab-secreting anti-RV intestinal B cells. The frequency of total IgA$^+$ ASCs as a proportion of total intestinal B cells was 35.2% (10.0 to 61.6%). The frequency of VP6-specific IgA$^+$ ASCs as a proportion of total IgA$^+$ ASCs was 0.16% (0.03 to 0.37%) (Fig. 2C).

Barcode-based sequencing of RV TLP-reactive IgA$^+$ intestinal ASCs

A total of 1026 IgA$^+$ ASCs were single cell–sorted, and complementary DNAs (cDNAs) from individual Ig mRNAs were synthesized to incorporate well- and plate-specific barcodes (23). The barcodes were used to pair heavy-chain (HC) and light-chain (LC) Ab sequences derived from the same B cell. Paired *IGHV/IGLV* sequences (821) were retrieved from the five donors (~80% efficiency). The median number of paired Ab sequences recovered per donor was 207 (range, 82 to 227). Sequences of the HCs and LCs from each Ab were used to construct dendrograms to visualize Abs with identical germline *IGHV* and *IGLV* genes in each donor (Fig. 3) (23). Briefly, HC and LC variable regions (FR1 to FR4) from each cell were concatenated, the sequences were sorted by *IGHV* gene family, and concatenated sequences were aligned and clustered within each family. Clonal families and singletons were defined as described (23). Clonally related Abs were identified at an overall frequency of 29% of paired sequences from all donors (9 to 60% in individual donors) (Fig. 3).

Determination of the specificity of human mAbs

Thirty-four *IGHV/IGLV* paired sequences from clonal families and 27 singletons were expressed as recombinant IgG mAbs with an expression efficiency of roughly 73% (Fig. 3). Abs were selected for expression from each subject by identifying an even distribution of clonal family sequences from across *IGHV* and *IGLV* gene families, proportionally to the gene family's prevalence. Where clonal families were not present in sufficient numbers in a given subject or gene family, singletons were selected to represent the family. From the available clonal/singleton sequences in each category, preference was given to sequences with *IGHV* mutations from germ line close to the median number and to sequences represented by the highest number of sequencing reads. Each mAb was screened by enzyme-linked immunosorbent assay (ELISA) to determine its binding reactivity to recombinant VP2/VP6 (rhesus RV) DLPs, human Wa strain RV-derived DLPs to ascertain binding reactivity against simian and human VP6, respectively, and to replication-competent CDC-9 TLPs (G1P[8]) that were used to identify RV-reactive B cells by fluorescence-activated cell sorting (FACS). Anti-RV VP4 or VP7 mAbs were defined as those binding to TLPs but not DLPs. Anti-VP6 mAbs were defined as those binding to purified DLPs whether or not they bound to TLPs (Table 1). Thirty-two of the 61 expressed mAbs bound to TLPs, but not DLPs, and were denoted VP4- or VP7-specific. One mAb bound to both TLPs and DLPs and was denoted VP6-specific. Therefore, 54% of the selected ASCs encoded Ab sequences that were RV-specific. Of the 33 RV-specific mAbs, 22 were derived from clonal families and 11 were singletons (Fig. 3 and Table 1).

The binding reactivity of the VP4/VP7-reactive recombinant mAbs was examined using a set of biochemistry and virology approaches including immunostaining of RV-infected African green monkey kidney epithelial (MA104) cells, immunostaining of baculovirus (BV)–infected Sf9 cells expressing recombinant RV proteins, ELISA binding to the recombinant VP8* or VP5*, and immunoprecipitation of recombinant RV proteins expressed in vitro (Table 1 and tables S2 and S3) (24). All 32 VP4- or VP7-specific mAbs bound to Wa (G1P[8])–infected cells (table S3). Twenty-five of these mAbs also bound to DS1 (G2P[4])–infected cells. Several mAbs displayed weak binding to cells infected with nonhuman simian, bovine, or porcine RVs (table S3). Hence, most isolated VP4/VP7-

specific mAbs displayed some degree of heterotypic binding to different RV serotypes. Six VP4/VP7-specific mAbs bound only to cells infected with Wa RV including three of the four VP7 mAbs (table S3).

The protein binding specificity of the mAbs was determined using Sf9 cells expressing recombinant RV VP4s, VP7 (Wa G1), or VP6 (rhesus rotavirus) (table S3) (25). Of the 32 anti-VP4/VP7 mAbs, 28 bound to recombinant VP4 and 4 bound to recombinant VP7 (Table 1 and table S3). The binding specificity among the 28 anti-VP4 mAbs varied considerably (table S3). The single DLP-binding mAb (#10, Table 1, bound to VP6. Further resolution of the binding specificity of anti-VP4 mAbs revealed that most (22 of 28) bound to recombinant VP8* (table S3), and most of these bound only to the VP4s derived from Wa alone or Wa and DS1. Four of the anti-VP4 mAbs bound to recombinant VP5* (Table 1 and table S3) (26). The VP8* versus VP5* specificity of non-neutralizing mAb #62 was unable to be determined (Table 1 and table S3).

In vitro neutralizing activity of VP4- and VP7-specific intestinal mAbs

The VP4- and VP7-binding recombinant mAbs were examined by in vitro neutralization (Table 2). Eight of the 32 (25%) RV surface protein–reactive mAbs efficiently neutralized at least one of these RV strains in vitro, whereas two VP8* mAbs (#9 and #19) had only minimal neutralization activity (Table 2). Three of the eight strongly neutralizing mAbs (#27, #46, and #57) were VP7-specific, four were VP4-specific (#2, #30, #33, and #41), and one was VP8*-specific (#47) (Tables 1 to 3). Other than mAb #47, none of the 22 VP4-directed mAbs that bound to a recombinant VP8* demonstrated efficient neutralizing activity, as defined by a minimum neutralizing concentration of less than 78.1 ng/ml, although two (#9 and #19, Table 2) demonstrated minimal plaque reduction potency (Table 2 and Fig. 4).

Homotypic neutralizing mAbs were defined as mAbs for which the minimum neutralization concentration to a single serotype (G or P) was >10-fold lower than to any other serotype. Heterotypic mAbs were defined as those with minimum neutralization concentration within 10-fold for two or more distinct P or G serotypes. Two of the eight potent neutralizing Abs were homotypic: VP7-directed mAbs #27 and #46. The remaining six potent neutralizing Abs all had heterotypic activity: anti-VP5* mAbs #2, #30, #33, and #41; anti-VP8* mAb #47; and anti-VP7 mAb #57 (Table 2). Several serotypically uncommon human RV strains 69M (G8P[10]), 116E (G9P[11]), and #321 (G10P[11]) were not neutralized by any of these mAbs at concentrations up to 625 ng/ml. The two weakly neutralizing VP8*-reactive mAbs (#9 and #19) only neutralized Wa and WI61 and did not neutralize 100% of Wa or WI61 even at high concentrations (Table 2). Analysis of the molecular features of all 10 neutralizing mAbs did not reveal any preferential skewing in the molecular profiles of the variable regions. In contrast, the mAbs had distinct VH and VL gene segment usage and CDRH3 amino acid sequence and length (table S4).

Determination of the functional interactions between VP8* and VP5* mAbs

To further investigate the functional relevance of the weakly or non-neutralizing mAbs to VP8*, we examined whether these mAbs could modify the neutralization capacity of the

anti-VP5* or anti-VP8* mAbs. None of the 20 non-neutralizing VP8* mAbs (Table 1) enhanced or inhibited VP5*, VP8*, or VP7 mAb-mediated neutralization. However, both weakly neutralizing VP8* mAbs, #9 and #19 for Wa (Table 2), reduced the ability of the VP5* mAb #41 and VP8* mAb #47, but not any of the VP7 mAbs, to neutralize, even at their highest concentration. The minimum concentration of mAb #9 required for inhibition of neutralization by mAb #41 was 4.9 ng/ml. Further decrease in the concentration of mAb #9 had neither neutralization inhibition activity nor significant focus reduction activity (Fig. 4). In contrast, the two neutralizing VP5* mAbs, #33 for ST3 and #41 for DS1, did not inhibit the neutralization of these specific viral strains by the potent neutralizing mAbs #41 or #30, respectively. These results suggest that the neutralization inhibition phenomena is restricted to the weakly neutralizing Abs against VP8* and not those against VP5*.

In vivo homotypic and heterotypic neutralizing activity of VP4- and VP7-specific intestinal mAbs

The ability of mAbs to protect against RV-induced diarrhea in vivo was examined in a suckling mouse model using a simian RV (RRV, G3P[3]), a human RV VP7-RRV monoreassortant DxRRV (G1P[3]) with the human G1 VP7 on an RRV genetic background, a monoreassortant SB1A × DS1 (G5P[4]) with a human P[4] VP4 on a porcine SB1A genetic background, and human Wa RV (G1P[8]) as challenge strains (11). VP7-specific mAb #27 (G1-specific) prevented DxRRV-induced but not RRV-induced diarrhea (Fig. 5A). VP7-directed heterotypic mAb #57 efficiently protected suckling mice against both RRV- and DxRRV-induced diarrhea (Fig. 5B). Heterotypic VP5* mAb #41 had a protective efficacy of 67% against the P[4] SB1A × DS1 monoreassortant and a 100% protective efficacy against the Wa strain (Fig. 5C). Thus, the anti-VP7 mAb #27 was able to inhibit RV-induced diarrhea in a VP7 serotype-specific manner, whereas anti-VP7 mAb #57 and anti-VP5* mAb #41 inhibited RV-induced diarrhea in a heterotypic manner.

Identification of escape mutation sites of RV neutralizing human mAbs

To identify potential neutralizing mAb binding sites on VP4 or VP7, we first cocultured mAb #41 or #47 with Wa and mAb #27 or #57 with DxRRV and isolated respective escape variants. To identify the escape mutation sites for various neutralizing mAbs, we sequenced VP4 of Wa RV escape variant (denoted Wa41v-1–1) that is resistant to neutralization by mAb #41 (Table 3) (27). Wa41v-1–1 had a single-nucleotide mutation from cytosine to adenine at position 1175, resulting in a substitution from alanine to glutamic acid at amino acid 392. This mutation maps to a previously identified putative membrane interaction loop of VP5* (7, 28). Notably, Wa41v-1–1 also resisted neutralization by mAb #33, but not by mAb #47, suggesting that mAbs #33 and #41 bind to related epitopes on VP5*. mAb #47, the only VP8* mAb identified that had potent neutralization activity, selected an escape mutation at amino acid 123 in VP8*, a site near the tip of the VP4 spike and not previously identified as an escape mutation site (Table 3). The escape phenotypes for the other two VP5*-specific mAbs (#2 and #30) have not yet been identified (Table 2). VP7-specific mAb #57 selected an escape mutation at amino acid 126, a site not previously associated with VP7 escape mutations. This mutation did not lead to escape from neutralization by the two homotypic VP7 mAbs (#27 and #46) (Table 3). mAb #27 selected an escape mutation at amino acid 151 in VP7, a site previously linked to Ab escape. This mutation also led to

escape from neutralization by the other homotypic G1-specific mAb #46, but not from heterotypic mAb #57.

DISCUSSION

RVs, including human RVs, are antigenically and serotypically diverse, suggesting that broadly protective immunity requires immunization or infection with multiple antigens, such as is the case for influenza viruses. However, it has been observed that young children develop substantial resistance to severe RV illness after one or two natural infections or monotypic RV vaccination (2). The mechanisms underlying this heterotypic resistance to multiple RV serotypes have remained unknown for more than 30 years. This is due, in part, to the fact that previous attempts to characterize human VP4- or VP7-specific B cells have been unsuccessful because only very young children are susceptible to RV illness, and it is difficult to acquire acute-phase plasmablast-rich blood from this vulnerable population. Because RV TLPs uncoat during storage and/or experimental manipulations, attempts to isolate anti-VP4 or anti-VP7 B cells using recombinant TLPs as a sorting ligand resulted in the selection of numerous anti-VP6 B cells. Here, the use of a naturally occurring, stable TLP-forming human RV strain (CDC-9), optimized labeling and sorting conditions and small bowel resections as an ample source of human IgA B cells, enabled an excellent discovery rate of 52% (32 of 61) for anti-RV VP4 and VP7 Igs. The isolation of only one VP6 Ig attested to the stability of the CDC-9–Cy5 construct during B cell isolation. Using the CDC-9–Cy5 TLP as bait in flow cytometry sorting coupled with barcode-based deep sequencing of Ig repertoires, mAb expression, and serologic and functional characterization, we demonstrate that broadly cross-neutralizing Igs produced by enteric B cells and directed at VP4 (VP5*), VP7, and VP8* represent one potential mechanism for the evolution of broadly cross-reactive immunity in people induced by single natural infection or monotypic RV vaccination.

One of the principal findings of this work is that heterotypic, but not homotypic, Igs against VP5* are generated by infection, and these Igs are capable of mediating broad-based protection against serotypically distinct RV strains. On the basis of the 10 neutralizing mAbs analyzed in this study, it appears that VP5*-directed heterotypic responses are more frequent than heterotypic responses to VP8* or VP7 and homotypic responses to VP5*, VP8*, or VP7. Because of the limited number of neutralizing mAbs identified in total and the fact that only a single neutralizing mAb was identified in four of the five adults analyzed, additional neutralizing mAbs from adults and children will need to be characterized to determine whether heterotypic responses to VP5* are the dominant protective neutralizing Abs induced after natural infection or monotypic vaccination in young children.

Most of the VP4-reactive mAbs (virtually all directed at VP8*) were inactive in traditional neutralization assays and did not prevent RV-associated diarrhea in suckling mice. In contrast, all four of the isolated anti-VP5* mAbs were neutralizing, and all demonstrated heterotypic reactivity both in vitro and in vivo functional protection assays. RV neutralizing epitopes have been mapped to both the VP5* and VP8* domains of VP4 using mAbs primarily isolated from parenterally immunized mice (29, 30). The VP8*-directed murine mAbs were generally type-specific, consistent with the greater degree of sequence

divergence in this region of the VP4 molecule. The only previously isolated human anti-VP4 mAbs, both of which were selected by a neutralization screening assay, were directed at VP8*, and both of these demonstrated heterotypic specificity (31), similar to the one potent VP8* neutralizer isolated in this study (#47). VP5*-directed murine mAbs have been less commonly isolated but have demonstrated more cross-reactive serologic specificity (7). The cross-reactivity of anti-VP5* Abs is consistent with the sequence conservation and functional constraints on this region of molecule (28). The fact that all the VP5*-directed Abs isolated here had the ability to restrict RV replication would suggest that, like VP7, much of the VP5* antigenic surface, including the area targeted by the heterotypic VP5* neutralizing mAb #41 that is exposed on TLPs, plays an important role in mediating viral entry and initiating infection. The precise epitope specificity of the VP5* mAb binding and mechanisms of the homotypic versus heterotypic neutralization warrant structural studies using these and other human origin neutralizing versus non-neutralizing mAbs and homotypic versus heterotypic mAbs specific for VP5* of various RV strains.

We observed that heterotypic Igs against VP7 can also be generated after RV infection. Although only a few mAbs were isolated, anti-VP7 heterotypic responses were identified at half the frequency as anti-VP7 homotypic responses. Strong homotypic responses were only observed to VP7 and not to VP4. Neutralizing Abs represented a limited subset of the immune repertoire generated to VP4 but a larger proportional component (three of four) of VP7-directed mAbs. The four anti-VP7 mAbs identified are too few to predict what proportion of the human immune response to virion-associated VP7 restricts RV replication, but these initial data suggest that most Abs that bind to the trimeric VP7 found on the RV surface inhibit viral replication (32).

Our results also indicate that VP8* is not a frequent target of either heterotypic or homotypic protective Abs in humans. This finding is in stark contrast to published studies where murine mAbs raised against animal RVs identified VP8* as a frequent target of neutralizing Abs (11, 33). Vaccine studies have demonstrated that a truncated VP8* subunit protein vaccine candidate elicits RV neutralizing Ab responses in animal models (34) and boosts neutralizing Ab titers in RV-experienced adults when administered parenterally (35). Twenty of the 23 individual anti-VP8* Abs isolated in this study had no activity in traditional in vitro neutralization assays or in passive protection challenge experiments in suckling mice. In addition, the neutralizing activity of two of the three VP8*-directed mAbs that reduced Wa replication was very limited.

Note that all 21 of the non-neutralizing or minimally neutralizing VP8* mAbs bound to bacterially expressed VP8*, indicating that the epitopes defined by these non-neutralizing mAbs were unlikely to require posttranslational eukaryotic modification for proper folding. The one potent neutralizing VP8* mAb (#47) only bound to VP8* when present on the virion or when expressed as part of the full-length VP4 molecule, suggesting that it reacted with a more conformation-dependent epitope not well expressed on the recombinant VP8*. Future structural studies will be needed to confirm these conjectures and to better define the reason for mAb #47’s restrictive binding dependence. Whether the large number of selected VP8* mAbs that lacked neutralization capacity represent a sampling error due to the limited number of adults and Abs examined, an unknown bias in our B cell selection strategy, or

whether VP8* neutralizing epitopes are differentially presented in the intestinal milieu of people, remains unknown.

The two VP8* directed mAbs, which expressed minimal neutralizing capacity, also have the capacity to partially inhibit the neutralization potency of other VP5*-specific and VP8* (but not VP7)–specific neutralizing mAbs in vitro. It remains unknown whether this in vitro effect has relevance to protection in vivo. It will also be important to determine whether any anti-VP8* mAbs, despite their lack of in vitro neutralizing activity, are able to interfere with RV binding to specific glycoarrays, which might reflect the enterocyte binding specificity of specific RV strains (36). The primarily negative results observed here with human VP8*-directed mAbs suggest some caution regarding the potential of recombinant VP8* to function as an effective human RV vaccine candidate.

The precise location of the binding sites of all the heterotypic human VP5* mAbs described here and their mechanism of neutralization are beyond the scope of this study. Such Abs are unlikely to function by inhibiting viral binding but are probably involved in restricting cell entry (33). Previous studies using murine mAbs identified a binding site that relied on amino acid 393 of RRV as a critical location for VP5*-directed heterotypic mAbs (11). This finding is consistent with the assignment of a mAb #41 escape mutation to amino acid 392 of the Wa RV strain. Given that escape mutations at amino acid 392 also reduced the neutralizing activity of mAb #33, it seems likely that this mAb binds to an identical or related epitope. Direct evidence of the involvement of this epitope in mediating protection in children has been demonstrated (37). Further analysis will be needed to identify the binding regions on VP5* of mAbs #2 and #30. Recombinant VP5* antigens that interact with any or several of these potent heterotypic mAbs would be promising candidates for novel third-generation RV vaccines needed in developing countries where live, orally delivered RV vaccines demonstrate reduced efficacy compared to developed countries (2). Parenterally administered subunit RV vaccines have the potential to be safer and to overcome inhibition of vaccine virus growth by transplacentally acquired or breast milk Ab, interference by other pathogens in the gut and gut-associated factors, such as enteropathy, commonly observed in developing countries (38). The induction of high Ab titers by the adjuvanted parenteral injection of nonreplicating RV vaccines may result in mucosal protection mediated by the induction and transfer of Abs into the gut.

With regard to VP7 epitope mapping, the single heterotypic VP7 mAb we identified selected an escape mutation at amino acid 126, whereas the two homotypic VP7 mAbs lost reactivity to a variant with a mutation at amino acid 151. Structural studies will be needed to determine the precise binding sites and relationships between the heterotypic and homotypic human VP7 mAbs.

In summary, our findings provide a plausible mechanism to the fundamental question regarding how heterotypic immunity to RV illness is generated after natural infection or monotypic vaccination. It appears that VP7, VP5*, and VP8* each have antigenic regions capable of eliciting potent heterotypic neutralizing responses. One of the limitations of this study was the small number of neutralizing mAbs that were analyzed. In our analysis of 10 neutralizing mAbs from five donors, such potent heterotypic mAbs to VP5* were isolated

from three of five subjects and heterotypic reactivity was the most common type of VP5* reactivity observed, whereas one of three isolated anti-VP7 mAbs from one subject also exhibited a potent heterotypic neutralization phenotype. On the other hand, only 1 of 23 VP8*-directed mAbs exhibited potent heterotypic reactivity. These findings suggest that a vaccine containing or expressing authentic VP4, VP8*, VP7, or more likely VP5*, represents a promising approach for the development of third-generation, nonreplicating RV vaccine candidates. Identification of the regions of VP5* that are the targets of these heterotypic neutralizing Abs would aid in the design of more effective, next-generation vaccines needed to reduce the high disease burden attributed to RV in developing countries.

METHODS

Study design

The study was designed as an exploratory study to isolate and characterize Abs specific to RV VP4 and VP7. Five adult donors undergoing bariatric surgery were included. B cells from the entire tissue resection obtained from each donor were analyzed, and TLP-binding IgA^+ ASCs were single cell–sorted for paired *IGHV/IGLV* sequencing, mAb expression, and functional characterization.

Human subjects

Proximal jejunum tissue resections were obtained from adults undergoing bariatric surgery at the Stanford Hospital in accordance with approved institutional review board protocols (protocol ID #1726). Written informed consent was obtained from all patients before inclusion in this study. Subjects with chronic viral infections or acute gastroenteritis at the time of surgery were excluded.

Isolation of B cells from jejunum tissue

Viable B cells were isolated from jejunum resections within 2 hours of surgery as described (20). Briefly, tissues were digested for 1 hour at 37°C with 0.26 Wünsch units/ml Liberase TL (Roche). Intestinal B cells were enriched using EasySep Human B cell Enrichment Kits without CD43 depletion (STEMCELL Technologies) according to the manufacturer's instructions.

RV strains, propagation, and preparation of TLPs, DLPs, and VLPs

RVs (table S3) were grown in Vero cells (American Type Culture Collection) in the presence of trypsin (39). RV TLPs were purified from MA104 cell lysates as described (40). DLPs were prepared by treating TLPs with 5 mM EDTA for 20 min at 37°C. VP2–enhanced green fluorescent protein (eGFP)/VP6 particles were prepared as described (41). TLPs (CDC-9) were labeled with Cy5 as described (42) with modifications. TLPs (100 μg) were washed with 10 mM Hepes (pH 8.2), 5 mM $CaCl_2$, and 140 mM NaCl, labeled at 4:1 molar ratio of Cy5 monoreactive dye (GE Healthcare) to TLPs at room temperature for 1 hour followed by the addition of tris-HCl (pH 8.8) to a final concentration of 50 mM. Labeled viruses were purified by dialysis using Amicon Ultra Centrifugal filter unit (Millipore). The integrity of TLP-Cy5 was determined by electron microscopy (43).

Flow cytometry

Murine hybridomas specific for VP6 (1e11), VP4 P[8] (1a10) or P[3] (7a12), VP7 G1 (5e8) or G3 (159) (18, 21), or enriched human B cells were stained with TLP-Cy5 (2 μg) for 45 min on ice as described (20) with modifications. Intestinal B cells were stained with LIVE/DEAD Fixable Aqua Dead Cell Stain Kit (Life Technologies) for 20 min. The cells were washed and stained with a cocktail of fluorescently labeled Abs (table S1) for 30 min at 4°C. IgA^+ ASCs were single cell–sorted into a 96-well polymerase chain reaction (PCR) plate using the BD FACSAria III. A total of 200,000 events were acquired per sample. Data were analyzed using Cytobank.

Enzyme-linked immunospot

The frequencies of intestinal IgA^+ ASCs and $VP6^+$ IgA^+ ASCs were determined by ELISPOT as described (20). Briefly, 96-well plates (Millipore) were coated with affinity-purified goat anti-human IgA + IgG + IgM (H + L) (KPL) at a concentration of 4 μg/ml. Wells were coated with phosphate-buffered saline (PBS) as a negative control. Plates were incubated overnight at 4°C and blocked for 2 hours at 37°C with complete medium before use. B cells were suspended in complete medium containing peroxidase-conjugated goat anti-human IgA (Sigma-Aldrich), distributed in ELISPOT plates, and incubated for 4 hours at 37°C in 5% CO_2. Plates were washed and developed with 3-amino-9-ethylcarbazole (AEC) substrate (Vector Laboratories). The total ASCs per well was determined by counting the spots using the ImmunoSpot Analyzer (Cellular Technology Limited). Background ASCs detected in the wells coated with PBS were subtracted from the quantities of ASCs in treated wells.

Barcode-based sequencing of paired *IGH/IGL* genes

Reverse transcription and PCR with well-ID and plate-ID oligo-nucleotide barcode adaptors (which together serve as cell barcodes) were performed (23). Amplified DNAs were pooled, purified with AMPure XP beads (Beckman Coulter), and sent to Roche for 454 sequencing. Compound barcode assignment, assembly of sequences, V(D)J and clonal assignment, and clustering of sequences were performed (44). Original nucleotide sequences were submitted to GenBank. IMGT/HighV-Quest data were read into R, and B cells with shared HC VJ and LC VJ gene segments were clustered (table S6). Within these groups, CDR3 amino acid sequences were compared using the string-dist package to calculate the Levenshtein distance. Clonal families were defined as sharing HC and LC VJ genes and having a CDR3 amino acid Levenshtein distance of ≤3 for both. Dendrograms of the paired IGH/IGL sequences were produced as described (22, 45) by *IGHV*-anchored MUSCLE alignment and PHYML clustering of concatenated IGH/IGL variable regions from each B cell. Trees were visualized using the ete2 module in Python (45).

Cloning and expression of recombinant Abs

Ab cloning and expression were performed as described with modification (23). V(D)J gene regions from Iga HCs and VJ regions from kappa or lambda light chains were synthesized (Integrated DNA Technologies) and inserted into pFUSE-CHIg-hG1 (IgG1) and pFUSE2-CLIg-hK (IgK) or pFUSE2-CLIg-hL2 (IgL) expression vectors (InvivoGen) using the Cold

Fusion Cloning Kit (SBI). Plasmids encoding HC and LC V(D)J and VJ inserts were cotransfected into Expi293T cells (Life Technologies).

Enzyme-linked immunosorbent assays

The quantity of total Ig was assessed in transfection supernatants using the Human IgG ELISA kit (ZeptoMetrix). Binding reactivity was determined using TLPs (CDC-9), virus-like particles (VLPs) VP2-eGFP/VP6, bacterially expressed VP8* conjugated to tetanus toxoid (PATH), or VP5* (1 μg/ml) as capture antigens and detection of bound mAb using goat anti-human IgG horseradish peroxidase (KPL) (19).

Immunostaining

Immunostaining was performed as described (25) using Sf9 cells infected at a multiplicity of infection (MOI) of 0.1 with recombinant BVs expressing VP7 (G1) or VP4 (Ku, DS1, 1076). Infected Sf9 cells were fixed with 10% formalin (Sigma-Aldrich) for 30 min at room temperature and permeabilized with 1% Triton X-100 (Sigma-Aldrich) in 10 mM tris, 100 mM NaCl, and 1 mM $CaCl_2$ (pH 7.4) for 2 min at room temperature. mAbs were serially diluted and incubated for 1 hour at 37°C. mAbs that bound to specific BV-infected Sf9 cells were detected with peroxidase-conjugated goat anti-human IgG (KPL), followed by incubation with AEC substrate (Vector Laboratories). The endpoint immunostaining concentration was assigned as the highest dilution at which cell staining could be detected using an inverted microscope. All samples were run in duplicate, and each assay was repeated twice.

Immunoprecipitation

MA104 cells were infected with human Wa strain at MOI of 3 for 16 hours. Total RNA was isolated using the RNeasy Mini Kit (Qiagen), and cDNA was prepared using High-Capacity cDNA Reverse Transcription Kit (Applied Biosystems). VP4, VP5*, and VP8* coding sequences were amplified using Phusion polymerase (New England Biolabs), and the primers are listed in table S5. Amplified sequences were cloned into pCMV6-XL6 vector (OriGene) containing SP6 promoter using Kpn I and Hind III restriction sites.

VP4, VP5*, and VP8* proteins were translated in vitro using TNT Quick Coupled Transcription/Translation Systems (Promega) with rabbit reticulocyte lysate and SP6 polymerase. The translated proteins or whole virus particles were mixed with human anti-RV mAbs and incubated overnight at 4°C with continuous mixing. The protein-mAb complexes were incubated for 1 hour at room temperature with PureProteome Protein A/G magnetic beads (Thermo Scientific) and precipitated using a magnetic field. The immune complexes were resolved in denaturing SDS–polyacrylamide gel electrophoresis and immunoblotted to polyvinylidene difluoride membrane. The membranes were probed with anti-VP5* IgG (HS-2). Immunoprecipitated proteins were visualized using ECL Plus Western blotting substrate (Thermo Scientific).

Virus neutralization assays

Virus neutralizations were performed as described (46) with recombinant mAbs (5 μg/ml) that were serially diluted and mixed with RVs (table S2) for 1 hour at 37°C. The mAb-virus

mixture was transferred to MA104 cell monolayers in a 96-well plate and incubated for 1 hour at 37°C in 5% CO_2 after which the mAb-virus mixture was removed, and the cells were washed twice and incubated overnight at 37°C with 100 μl of M199 media without serum or trypsin. The cells were fixed with 10% formalin for 30 min and permeabilized with 1% Triton X-100 for 2 min.

The cells were washed and incubated with polyclonal rabbit anti-RV IgG for 2 hours at 37°C followed by washing and a 1-hour incubation with peroxidase-conjugated goat anti-rabbit IgG (γ chain–specific) (Sigma-Aldrich). After the incubation, a color reaction was detected with the AEC substrate. The neutralization activity was defined as the highest dilution at which virus-positive foci were reduced by at least 50% compared to the wells that were not treated with mAb and was expressed as minimum neutralization concentration (nanograms per milliliter). All samples were run in duplicate, and each assay was repeated twice.

Mouse passive challenge studies

RVs were incubated with human anti-RV mAbs (5 μg/ml) for 1 hour at 37°C. The RV-mAb mixture was used to orally gavage 5-day-old 129/Sv suckling mice (Taconic Biosciences). Human anti-VP7 mAbs (#27 and #57) were mixed with RRV or a DxRRV monoreassortants containing a G1 VP7 on an RRV background, and human anti-VP4 mAb (#41) was mixed with Wa or a DS1xSB1A monoreassortant containing DS1 VP4 on an SB1A background. Six to 11 suckling mice were included per test group. The RV dose for each inoculum was 10^6 PFU. Mice were monitored for 4 days for diarrheal disease (table S7). All experiments were conducted in accordance with Stanford University and the VA Palo Alto Health Care System guidelines (protocol ID #GRH1397).

Isolation of mAb escape variant

Wa or DxRRV escape variants of the neutralizing mAbs #41, #47, and #57 were isolated as described (27). Briefly, parental strain Wa (10^6 PFU/ml) was incubated with mAb #41 or #47 (50 ng/ml), and parental strain DxRRV (10^7 PFU/ml) was incubated with mAb #57 (50 ng/ml) for 1 hour and added to MA104 cells for 1 hour. The inoculant was removed, and mAbs (50 ng/ml) were added back to cells and incubated for 5 to 6 days. The preparation was then plaque-purified on MA104 cells in the presence of mAbs. Putative mAb escape variants were plaque-purified twice. The viral RNA of putative mAb escape variants and parental Wa or DxRRV was obtained using TRIzol-chloroform extraction and converted to cDNA using High-Capacity Reverse Transcription Kit (Thermo Fisher). VP8* and VP5* fragments were amplified using Phusion high-fidelity polymerase (New England Biolabs, M0530) and the following primers: VP8*, 5′-ATGGCTTCACTCATTTATAGACAGC-3′ (forward) and 5′-TACTGGCCATGCACCTACTG-3′ (reverse); VP5*, 5′-CAAGTAACCGCACACACCAC-3′ (forward) and 5′-TCACAATTTACATTGTAGTATTAACTGTTCAAT-3′ (reverse). PCR products were gel-purified using Wizard SV Gel and PCR Clean-Up kit (Promega) and cloned into Zero Blunt TOPO PCR4 vector (Thermo Fisher, K270040) for Sanger sequencing. VP7 fragments were amplified from cDNA using the primers 5′-TAGCGGACACACTTTCACGG-3′ (forward) and 5′- TCCCATCAACGACATCCACT-3′ (reverse), and PCR products were purified and subjected to sequencing.

Effects of VP8* mAbs on VP5* mAbs in vitro neutralization activity

Wa was preincubated with VP8* mAb #9, #19, or #20 (200 ng/ml) for 1 hour at 37°C. The mixture was added to serially diluted VP5* mAb #41 or #47 for 1 hour at 37°C. The mixture of Wa, VP8* mAb, and VP5* mAb was added to MA104 cells for 1 hour at 37°C. This mixture was removed and cells were washed. M199 media without serum and trypsin were added back to cells for 16 hours. Plates were stained as in a neutralization assay (46). Neutralization titers of individual mAb (#9, #19, #41, or #47) against Wa were measured as controls. The results were presented as percentage of focus reduction at different mAb concentrations.

Statistics

One-way analysis of variance (ANOVA) and Tukey's multiple comparisons test were used to compare differences between multiple groups. P values <0.05 were considered significant. Analyses were performed using GraphPad Prism.

Supplementary Material

Refer to Web version on PubMed Central for supplementary material.

Acknowledgments:

We thank C. Zhang, Y. Wang, X. Che, and PATH for VLPs, CDC-9 TLPs, recombinant VP8*, and technical assistance and P. Dormitzer and M. Metruccio for critical review of the manuscript. **Funding:** This work was supported by NIH grants RO1 AI021362, R56 AI021362, U19 AI116484, and U19 AI090019 and VA Merit grant GRH0022. N.N. was supported by Stanford NIH-NCATS-CTSA UL1 TR001085 and Stanford Child Health Research Institute.

REFERENCES AND NOTES

1. Lanata CF, Fischer-Walker CL, Olascoaga AC, Torres CX, Aryee MJ, Black RE, Global causes of diarrheal disease mortality in children <5 years of age: A systematic review. PLOS ONE 8, e72788 (2013). [PubMed: 24023773]
2. Jiang V, Jiang B, Tate J, Parashar UD, Patel MM, Performance of rotavirus vaccines in developed and developing countries. Hum. Vaccin 6, 532–542 (2010). [PubMed: 20622508]
3. Fields BN, Knipe DM, Howley PM, Griffin DE, in Fields Virology (Wolters Kluwer Health/ Lippincott Williams & Wilkins, 2013), vol. 2, chap. 45, pp. 1347–1401.
4. Taniguchi K, Urasawa T, Kobayashi N, Ahmed MU, Adachi N, Chiba S, Urasawa S, Antibody response to serotype-specific and cross-reactive neutralization epitopes on VP4 and VP7 after rotavirus infection or vaccination. J. Clin. Microbiol 29, 483–487 (1991). [PubMed: 1709946]
5. Aoki ST, Settembre EC, Trask SD, Greenberg HB, Harrison SC, Dormitzer PR, Structure of rotavirus outer-layer protein VP7 bound with a neutralizing Fab. Science 324, 1444–1447 (2009). [PubMed: 19520960]
6. Padilla-Noriega L, Dunn SJ, López S, Greenberg HB, Arias CF, Identification of two independent neutralization domains on the VP4 trypsin cleavage products VP5* and VP8* of human rotavirus ST3. Virology 206, 148–154 (1995). [PubMed: 7530390]
7. Mackow ER, Shaw RD, Matsui SM, Vo PT, Dang MN, Greenberg HB, The rhesus rotavirus gene encoding protein VP3: Location of amino acids involved in homologous and heterologous rotavirus neutralization and identification of a putative fusion region. Proc. Natl. Acad. Sci. U.S.A 85, 645–649 (1988). [PubMed: 2829198]

8. Giammarioli AM, Mackow ER, Fiore L, Greenberg HB, Ruggeri FM, Production and characterization of murine IgA monoclonal antibodies to the surface antigens of rhesus rotavirus. Virology 225, 97–110 (1996). [PubMed: 8918537]

9. Mackow ER, Shaw RD, Matsui SM, Vo PT, Benfield DA, Greenberg HB, Characterization of homotypic and heterotypic VP7 neutralization sites of rhesus rotavirus. Virology 165, 511–517 (1988). [PubMed: 2457279]

10. Taniguchi K, Hoshino Y, Nishikawa K, Green KY, Maloy WL, Morita Y, Urasawa S, Kapikian AZ, Chanock RM, Gorziglia M, Cross-reactive and serotype-specific neutralization epitopes on VP7 of human rotavirus: Nucleotide sequence analysis of antigenic mutants selected with monoclonal antibodies. J. Virol 62, 1870–1874 (1988). [PubMed: 2452893]

11. Matsui SM, Offit PA, Vo PT, Mackow ER, Benfield DA, Shaw RD, Padilla-Noriega L, Greenberg HB, Passive protection against rotavirus-induced diarrhea by monoclonal antibodies to the heterotypic neutralization domain of VP7 and the VP8 fragment of VP4. J. Clin. Microbiol 27, 780–782 (1989). [PubMed: 2470774]

12. Taniguchi K, Maloy WL, Nishikawa K, Green KY, Hoshino Y, Urasawa S, Kapikian AZ, Chanock RM, Gorziglia M, Identification of cross-reactive and serotype 2-specific neutralization epitopes on VP3 of human rotavirus. J. Virol 62, 2421–2426 (1988). [PubMed: 2453680]

13. Dormitzer PR, Sun Z-YJ, Wagner G, Harrison SC, The rhesus rotavirus VP4 sialic acid binding domain has a galectin fold with a novel carbohydrate binding site. EMBO J. 21, 885–897 (2002). [PubMed: 11867517]

14. Velázquez FR, Matson DO, Calva JJ, Guerrero L, Morrow AL, Carter-Campbell S, Glass RI, Estes MK, Pickering LK, Ruiz-Palacios GM, Rotavirus infections in infants as protection against subsequent infections. N. Engl. J. Med 335, 1022–1028 (1996). [PubMed: 8793926]

15. Ruiz-Palacios GM, Pérez-Schael I, Velázquez FR, Abate H, Breuer T, Clemens SC, Cheuvart B, Espinoza F, Gillard P, Innis BL, Cervantes Y, Linhares AC, López P, Macías-Parra M, Ortega-Barría E, Richardson V, Rivera-Medina DM, Rivera L, Salinas B, Pavía-Ruz N, Salmerón J, Ruttimann R, Tinoco JC, Rubio P, Nuñez E, Guerrero ML, Yarzábal JP, Damaso S, Tornieporth N, Sáez-Llorens X, Vergara RF, Vesikari T, Bouckenooghe A, Clemens R, De Vos B, O'Ryan M; Human Rotavirus Vaccine Study Group, Safety and efficacy of an attenuated vaccine against severe rotavirus gastroenteritis. N. Engl. J. Med 354, 11–22 (2006). [PubMed: 16394298]

16. Bhandari N, Rongsen-Chandola T, Bavdekar A, John J, Antony K, Taneja S, Goyal N, Kawade A, Kang G, Rathore SS, Juvekar S, Muliyil J, Arya A, Shaikh H, Abraham V, Vrati S, Proschan M, Kohberger R, Thiry G, Glass R, Greenberg HB, Curlin G, Mohan K, Harshavardhan GVJA, Prasad S, Rao TS, Boslego J, Bhan MK; India Rotavirus Vaccine Group, Efficacy of a monovalent human-bovine (116E) rotavirus vaccine in Indian children in the second year of life. Vaccine 32 (suppl. 1), A110–A116 (2014). [PubMed: 25091663]

17. Higo-Moriguchi K, Akahori Y, Iba Y, Kurosawa Y, Taniguchi K, Isolation of human monoclonal antibodies that neutralize human rotavirus. J. Virol 78, 3325–3332 (2004). [PubMed: 15016854]

18. Burns JW, Siadat-Pajouh M, Krishnaney AA, Greenberg HB, Protective effect of rotavirus VP6-specific IgA monoclonal antibodies that lack neutralizing activity. Science 272, 104–107 (1996). [PubMed: 8600516]

19. Feng N, Lawton JA, Gilbert J, Kuklin N, Vo P, Prasad BVV, Greenberg HB, Inhibition of rotavirus replication by a non-neutralizing, rotavirus VP6–specific IgA mAb. J. Clin. Invest 109, 1203–1213 (2002). [PubMed: 11994409]

20. Nair N, Newell EW, Vollmers C, Quake SR, Morton JM, Davis MM, He XS, Greenberg HB, High-dimensional immune profiling of total and rotavirus VP6-specific intestinal and circulating B cells by mass cytometry. Mucosal Immunol. 9, 68–82 (2016). [PubMed: 25899688]

21. Greenberg HB, Valdesuso J, van Wyke K, Midthun K, Walsh M, McAuliffe V, Wyatt RG, Kalica AR, Flores J, Hoshino Y, Production and preliminary characterization of monoclonal antibodies directed at two surface proteins of rhesus rotavirus. J. Virol 47, 267–275 (1983). [PubMed: 6312065]

22. Benckert J, Schmolka N, Kreschel C, Zoller MJ, Sturm A, Wiedenmann B, Wardemann H, The majority of intestinal IgA^+ and IgG^+ plasmablasts in the human gut are antigen-specific. J. Clin. Invest 121, 1946–1955 (2011). [PubMed: 21490392]

23. Lu DR, Tan Y-C, Kongpachith S, Cai X, Stein EA, Lindstrom TM, Sokolove J, Robinson WH, Identifying functional anti-Staphylococcus aureus antibodies by sequencing antibody repertoires of patient plasmablasts. Clin. Immunol 152, 77–89 (2014). [PubMed: 24589749]
24. Shaw RD, Stoner-Ma DL, Estes MK, Greenberg HB, Specific enzyme-linked immunoassay for rotavirus serotypes 1 and 3. J. Clin. Microbiol 22, 286–291 (1985). [PubMed: 2993354]
25. Ishida S-I, Feng N, Tang B, Gilbert JM, Greenberg HB, Quantification of systemic and local immune responses to individual rotavirus proteins during rotavirus infection in mice. J. Clin. Microbiol 34, 1694–1700 (1996). [PubMed: 8784572]
26. Patton JT, Hua J, Mansell EA, Location of intrachain disulfide bonds in the VP5* and VP8* trypsin cleavage fragments of the rhesus rotavirus spike protein VP4. J. Virol 67, 4848–4855 (1993). [PubMed: 8392619]
27. Shaw RD, Vo PT, Offit PA, Coulson BS, Greenberg HB, Antigenic mapping of the surface proteins of rhesus rotavirus. Virology 155, 434–451 (1986). [PubMed: 2431540]
28. Dormitzer PR, Nason EB, Prasad BVV, Harrison SC, Structural rearrangements in the membrane penetration protein of a non-enveloped virus. Nature 430, 1053–1058 (2004). [PubMed: 15329727]
29. Offit PA, Shaw RD, Greenberg HB, Passive protection against rotavirus-induced diarrhea by monoclonal antibodies to surface proteins vp3 and vp7. J. Virol 58, 700–703 (1986). [PubMed: 2422398]
30. Kobayashi N, Taniguchi K, Urasawa S, Identification of operationally overlapping and independent cross-reactive neutralization regions on human rotavirus VP4. J. Gen. Virol 71, 2615–2623 (1990). [PubMed: 1701477]
31. Monnier N, Higo-Moriguchi K, Sun Z-YJ, Prasad BVV, Taniguchi K, Dormitzer PR, High-resolution molecular and antigen structure of the VP8* core of a sialic acid-independent human rotavirus strain. J. Virol 80, 1513–1523 (2006). [PubMed: 16415027]
32. Aoki ST, Trask SD, Coulson BS, Greenberg HB, Dormitzer PR, Harrison SC, Cross-linking of rotavirus outer capsid protein VP7 by antibodies or disulfides inhibits viral entry. J. Virol 85, 10509–10517 (2011). [PubMed: 21849465]
33. Ruggeri FM, Greenberg HB, Antibodies to the trypsin cleavage peptide VP8* neutralize rotavirus by inhibiting binding of virions to target cells in culture. J. Virol 65, 2211–2219 (1991). [PubMed: 1850007]
34. Fix AD, Harro C, McNeal M, Dally L, Flores J, Robertson G, Boslego JW, Cryz S, Safety and immunogenicity of a parenterally administered rotavirus VP8 subunit vaccine in healthy adults. Vaccine 33, 3766–3772 (2015). [PubMed: 26065919]
35. Wen X, Cao D, Jones RW, Li J, Szu S, Hoshino Y, Construction and characterization of human rotavirus recombinant VP8* subunit parenteral vaccine candidates. Vaccine 30, 6121–6126 (2012). [PubMed: 22885016]
36. Hu L, Crawford SE, Czako R, Cortes-Penfield NW, Smith DF, Le Pendu J, Estes MK, Prasad BVV, Cell attachment protein VP8* of a human rotavirus specifically interacts with A-type histo-blood group antigen. Nature 485, 256–259 (2012). [PubMed: 22504179]
37. Shaw RD, Fong KJ, Losonsky GA, Levine MM, Maldonado Y, Yolken R, Flores J, Kapikian AZ, Vo PT, Greenberg HB, Epitope-specific immune responses to rotavirus vaccination. Gastroenterology 93, 941–950 (1987). [PubMed: 2443417]
38. Jiang B, Gentsch JR, Glass RI, Inactivated rotavirus vaccines: A priority for accelerated vaccine development. Vaccine 26, 6754–6758 (2008). [PubMed: 18951937]
39. Wang Y, Vlasova A, Velasquez DE, Saif LJ, Kandasamy S, Kochba E, Levin Y, Jiang B, Skin vaccination against rotavirus using microneedles: Proof of concept in gnotobiotic piglets. PLOS ONE 11, e0166038 (2016). [PubMed: 27824918]
40. Bridger JC, Woode GN, Characterization of two particle types of calf rotavirus. J. Gen. Virol 31, 245–250 (1976). [PubMed: 180243]
41. Charpilienne A, Nejmeddine M, Berois M, Parez N, Neumann E, Hewat E, Trugnan G, Cohen J, Individual rotavirus-like particles containing 120 molecules of fluorescent protein are visible in living cells. J. Biol. Chem 276, 29361–29367 (2001). [PubMed: 11356839]

42. Carreño-Torres JJ, Gutiérrez M, Arias CF, López S, Isa P, Characterization of viroplasm formation during the early stages of rotavirus infection. Virol. J 7, 350 (2010). [PubMed: 21114853]

43. Jiang B, Wang Y, Glass RI, Does a monovalent inactivated human rotavirus vaccine induce heterotypic immunity? Evidence from animal studies. Hum. Vaccin. Immunother. 9, 1634–1637 (2013).

44. Tan Y-C, Blum LK, Kongpachith S, Ju C-H, Cai X, Lindstrom TM, Sokolove J, Robinson WH, High-throughput sequencing of natively paired antibody chains provides evidence for original antigenic sin shaping the antibody response to influenza vaccination. Clin. Immunol 151, 55–65 (2014). [PubMed: 24525048]

45. Huerta-cepas J, Dopazo J, Gabaldón T, ETE : A python environment for tree exploration. BMC Bioinformatics 11, 24 (2010). [PubMed: 20070885]

46. Hoshino Y, Wyatt RG, Greenberg HB, Flores J, Kapikian AZ, Serotypic similarity and diversity of rotaviruses of mammalian and avian origin as studied by plaque-reduction neutralization. J. Infect. Dis 149, 694–702 (1984). [PubMed: 6202807]

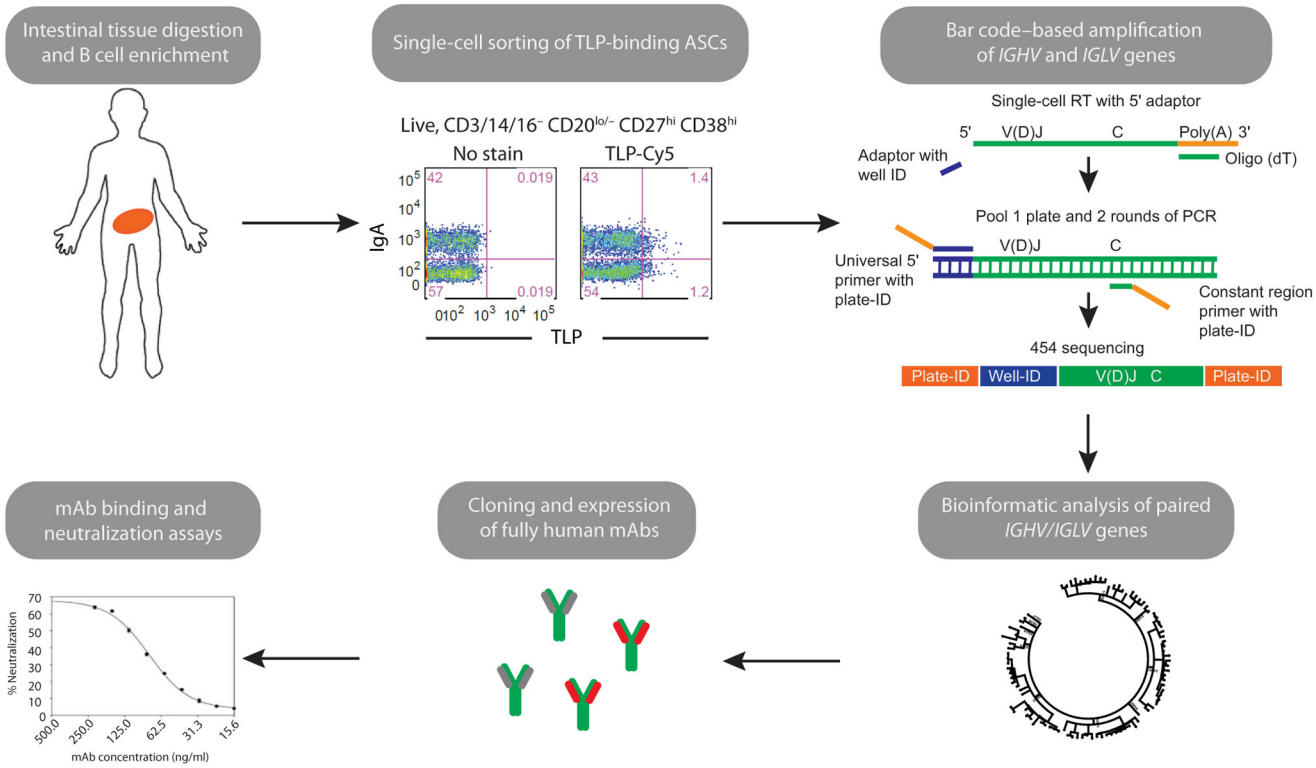

Fig. 1. Experimental workflow for identification of heterotypic and homotypic RV human mAbs.

Intestinal tissue from five bariatric surgery patients were isolated, B cells were enriched and live, TLP-binding IgA^+ ASCs were single cell–sorted. Barcode-based amplification of paired *IGHV/IGLV* genes from the same B cell was used to generate dendrograms of paired intestinal Ab sequences from each donor. Selected clonal and singleton Ab sequences were cloned and expressed as recombinant human mAbs. mAbs were characterized in terms of binding specificity to RV proteins and in vitro and in vivo neutralization capacities against distinct RV serotypes.

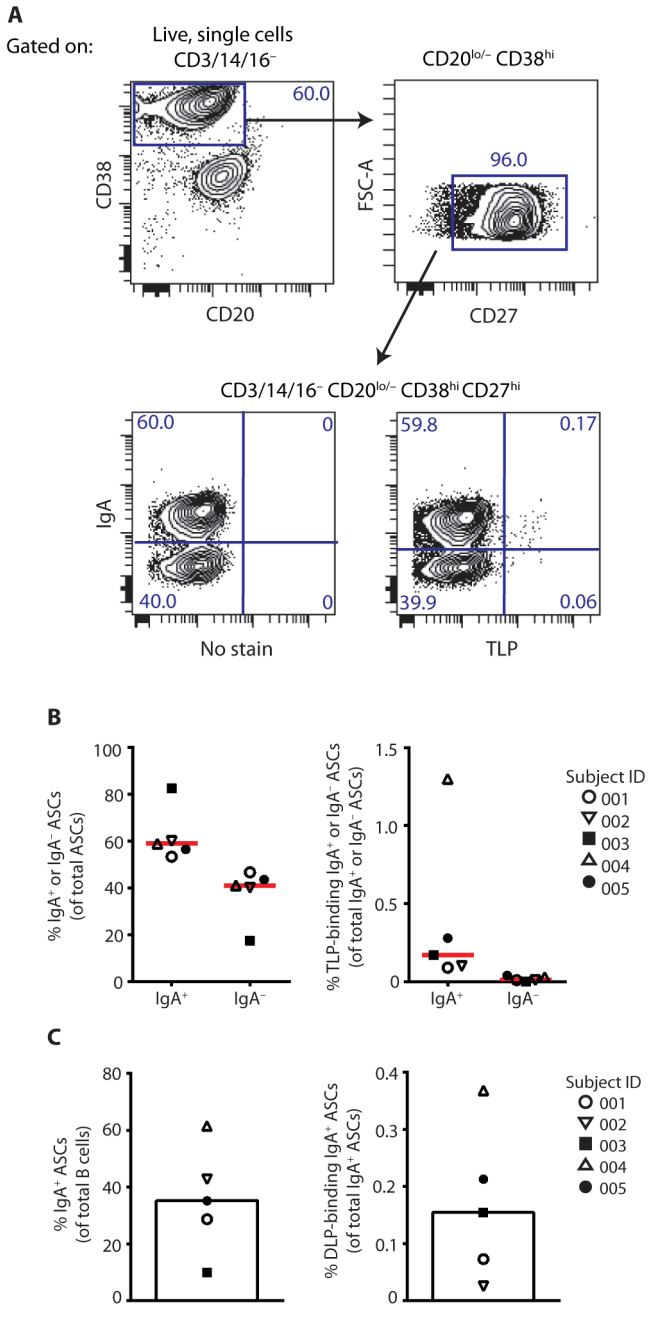

Fig. 2. Identification of TLP-binding intestinal ASCs in adult donors.

(A) CDC-9 TLP-binding intestinal ASCs were identified on the basis of $CD20^{lo/-}CD27^{hi}CD38^{hi}$ surface expression. Contour plots from a representative donor are shown. At least 200,000 events were acquired per sample. (**B**) The frequency of IgA^+ and IgA^- ASCs as a proportion of total intestinal ASCs (left) and of TLP-binding IgA^+ and IgA^- ASCs as a proportion of total IgA^+ and IgA^- ASCs (right), as determined by FACS in five donors. (**C**) Frequency of IgA^+ ASCs as a proportion of total intestinal B cells (left) and DLP-binding IgA^+ ASCs as a proportion of total IgA^+ ASCs (right), as determined by

ELISPOT. Symbols represent the frequencies of individual donors. Red lines and bars represent the median frequency.

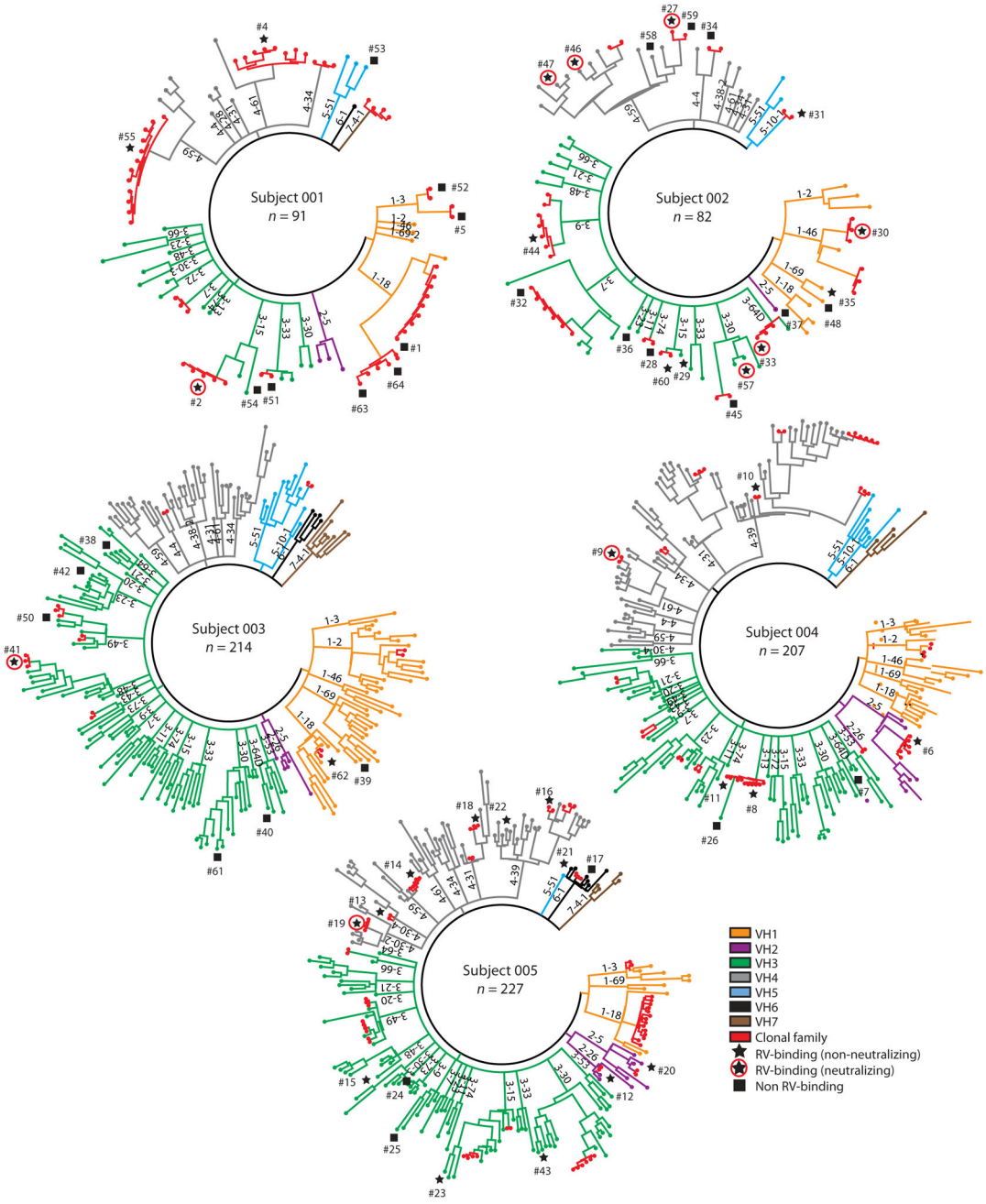

Fig. 3. Dendrograms of sorted RV TLP-reactive intestinal IgA$^+$ ASCs.

HC and LC dendrograms of sorted TLP-binding intestinal IgA$^+$ ASCs from five donors. Each peripheral node depicts sequenced VH and VL regions derived from a single cell. Red lines indicate clonal families. Ig V gene sequences that were selected for cloning and expression of recombinant mAbs are numbered. Stars denote Abs that bound to RV proteins. Circled stars denote neutralizing Abs. Squares denote Abs that did not bind to RV.

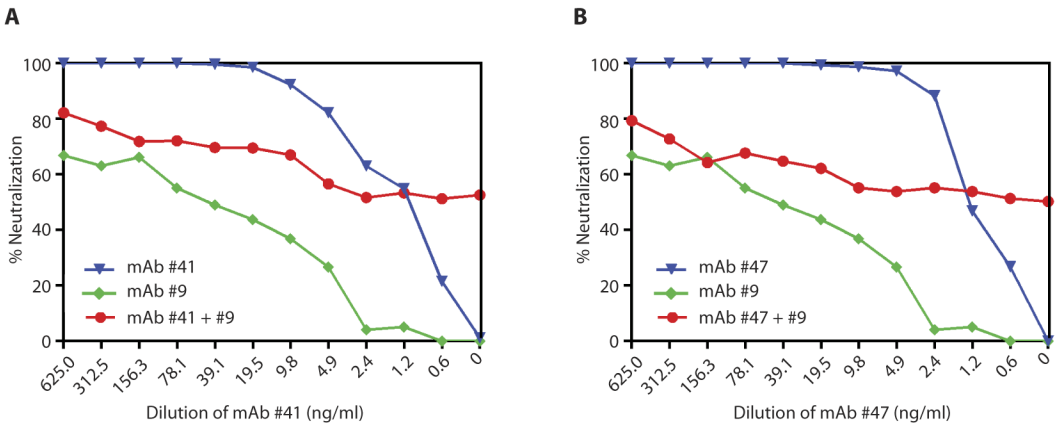

Fig. 4. Minimally neutralizing VP8* mAb interferes with the capacity of strong neutralizing VP5* or VP8* mAbs.

VP8* mAb #9 (200 ng/ml) was preincubated with Wa for 1 hour before the addition of potent neutralizing mAb #41 (VP5*) (**A**) or #47 (VP8*) (**B**) for an additional hour. The mixtures were then added to MA104 cells, and the neutralization assays were run as described.

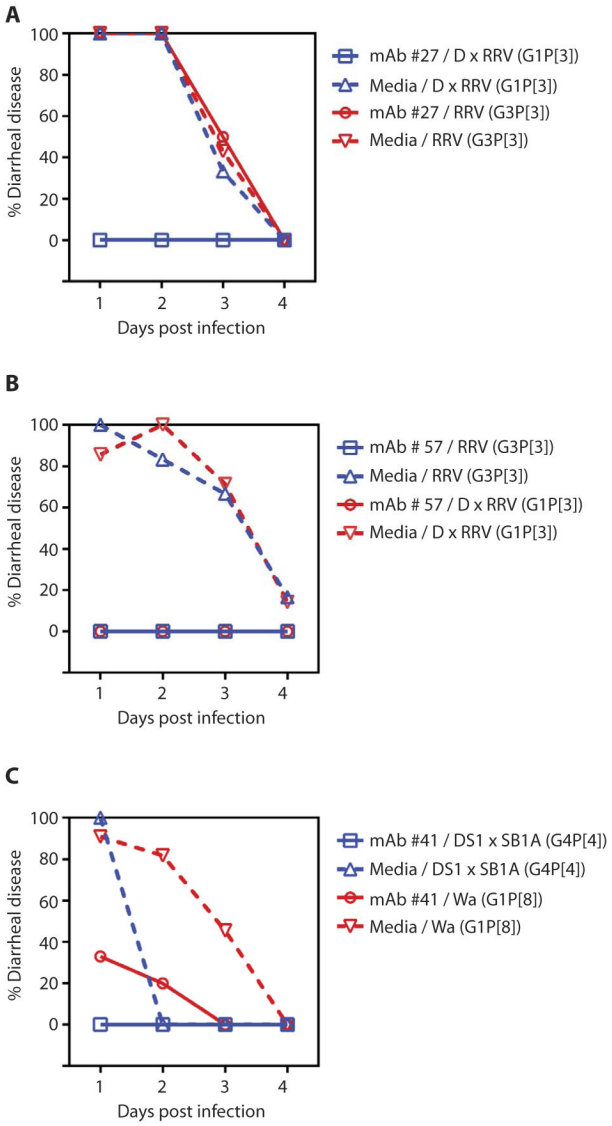

Fig. 5. Human mAbs mediate heterotypic and homotypic protection from RV-induced diarrheal disease in mice.

Five-day-old 129sv suckling mice (six to eight per group) were inoculated with 10^6 plaque-forming units (PFU) of indicated RV strains preincubated for 1 hour with human anti-VP7 (**A** and **B**) and anti-VP4 (**C**) mAbs (5 μg/ml) or with media. The percentage of pups with diarrhea up to 4 days after challenge is shown.

Sci Transl Med. Author manuscript; available in PMC 2018 December 31.

Table 1.

Summary of the protein specificity of RV-specific human recombinant mAbs. CF, clonal family; S, singleton; ND, VP5* or VP8* specificity not determined.

mAb no.	Subject ID	Viral protein specificity		Minimum concentration for TLP binding (ng/ml)	G serotype or P genotype binding activity	In vitro neutralization activity	Clonal family or singleton
2	001	VP4	VP5*	5.00	P[4] and P[8]	Yes	CF
30	002		VP5*	5.00	P[1], P[4], P[6], P[7], and P[8]	Yes	CF
33	002		VP5*	0.50	P[1], P[3], P[4], P[6], P[7], and P[8]	Yes	CF
41	003		VP5*	0.01	P[1], P[3], P[4], P[6], P[7], and P[8]	Yes	CF
4	001		VP8*	0.50	P[4] and P[8]	No	CF
6*	004		VP8*	5.00	P[4] and P[8]	No	CF
8	004		VP8*	0.05	P[4] and P[8]	No	CF
9	004		VP8*	0.01	P[4] and P[8]	Yes	CF
11	004		VP8*	0.01	P[4] and P[8]	No	CF
12	005		VP8*	0.05	P[4] and P[8]	No	CF
13	005		VP8*	5.00	P[8]	No	CF
14	005		VP8*	0.50	P[4] and P[8]	No	CF
15	005		VP8*	0.50	P[4] and P[8]	No	S
16	005		VP8*	0.01	P[4] and P[8]	No	CF
18	005		VP8*	0.05	P[4], P[6], and P[8]	No	CF
19	005		VP8*	0.05	P[4] and P[8]	Yes	CF
20	005		VP8*	0.01	P[4] and P[8]	No	S
21	005		VP8*	0.50	P[4] and P[8]	No	S
23	005		VP8*	50.00	P[4] and P[8]	No	S
29	002		VP8*	0.05	P[8]	No	S
31	002		VP8*	0.50	P[4] and P[8]	No	CF

mAb no.	Subject ID	Viral protein specificity	Minimum concentration for TLP binding (ng/ml)	G serotype or P genotype binding activity	In vitro neutralization activity	Clonal family or singleton
35	002	VP8*	0.50	P[1], P[4], P[7], and P[8]	No	S
43	005	VP8*	0.50	P[8]	No	S
44	002	VP8*	0.50	P[4] and P[8]	No	CF
55	001	VP8*	500.00	P[4], P[6], and P[8]	No	CF
60	002	VP8*	0.50	P[1], P[3], P[6], and P[8]	No	CF
47	002	VP8*	0.50	P[4] and P[8]	Yes	S
62	003	ND	5.00	P[4] and P[8]	No	CF
22	005	VP7	5.00	G1	No	S
27	002		0.01	G1,G5, and G9	Yes	CF
46	002		0.50	G1	Yes	S
57	002		0.50	G1,G2, G3, G4, and G5	Yes	S
10*	004	VP6	0.5†	G1, G2, G3, G4, G5, and G6	No	CF

*IgA. All other mAbs were expressed as IgG.

†Reacts with TLPs and DLPs. All other mAbs react only with TLPs.

Table 2.

Neutralization titers of RV-specific human mAbs against indicated RV strains and G and P types.—, no neutralizing activity.

mAb no.	Subject ID	RV protein specificity		RV strain neutralized (G,[P])*								Neutralizing activity
				Wa	DS1	RRV	ST3	OSU	NCDV	WI61	L26	
				G1P [8]	G2P [4]	G3P [3]	G4P [6]	G5P [7]	G6P [1]	G9P [8]	G12P [4]	
2	001	VP4	VP5*	—	4.9	—	—	—	—	4.9	625.0	Heterotypic
30	002		VP5*	312.5	1.2	—	9.8	78.1	312.5	1.2	—	Heterotypic
33	002		VP5*	4.8	—	39.1	39.1	156.3	156.3	—	—	Heterotypic
41	003		VP5*	0.6	39.1	9.8	4.9	78.1	19.5	2.4	4.9	Heterotypic
9	004		VPS*	78.1	—	—	—	—	—	312.5	—	Homotypic
19	005		VPS*	78.1	—	—	—	—	—	-	—	Homotypic
47	002		VPS*	1.2	4.9	—	—	—	—	78.1	—	Heterotypic
27	002	VP7		0.3	—	—	—	312.5	—	156.3	—	Homotypic
46	002			2.4	—	—	—	—	—	—	—	Homotypic
57	002			2.4	4.9	1.2	—	19.5	—	—	—	Heterotypic

*Minimum neutralizing concentration (nanograms per milliliter).

Table 3.

Neutralizing potency of different VP4 or VP7 mAbs against escape variants.

Parental virus/variants	Mutation site	VP4 Neutralizing mAbs*		
		#41	#33	#47
Wa		0.6	4.9	1.2
Wa41v-1–1	Amino acid 392 (A→E)	>625.0	>625.0	1.2
Wa41v-2–1	Amino acid 123 (G→D)	0.6	4.9	156.3
		VP7 Neutralizing mAbs*		
		#27	#57	#46
DxRRV		0.6	2.4	2.4
DRV57v-30–1	Amino acid 126 (D→N)	0.6	>625.0	2.4
DRV27v31–1	Amino acid 151 (D→H)	19.5	0.6	78.1

*Minimum neutralizing concentration (nanograms per milliliter).